Coherent Tunneling Adiabatic Passage with the Alternating Coupling Scheme

L M Jong, A D Greentree, V I Conrad, L C L Hollenberg and D N Jamieson

Centre for Quantum Computer Technology, School of Physics, University of Melbourne, VIC 3010, Australia

E-mail: lmjong@unimelb.edu.au

Abstract. The use of adiabatic passage techniques to mediate particle transport through real space, rather than phase space, is becoming an interesting possibility. We have investigated the properties of Coherent Tunneling Adiabatic Passage (CTAP) with alternating tunneling matrix elements. This coupling scheme, not previously considered in the donor in silicon paradigm, provides an interesting route to long-range quantum transport. We introduce simplified coupling protocols and transient eigenspectra as well as a realistic gate design for this transport protocol. Using a pairwise treatment of the tunnel couplings for a 5 donor device with 30 nm donor spacings, 120nm total chain length, we estimate the time scale required for adiabatic operation to be ~ 70 ns, a time well within measured electron spin and estimated charge relaxation times for phosphorus donors in silicon.

PACS numbers: 05.60.Gg, 73.63.Kv, 73.23.Hk, 03.67.-a

1. Introduction

The potential of silicon based proposals in particular to build upon and integrate with existing CMOS fabrication techniques makes them an attractive candidate for large scale quantum information processing architectures. Since the original proposal by Kane [1] for qubits based on the nuclear spins of ^{31}P donors in isotopically pure silicon ^{28}Si, other donor based systems have been suggested based on electron charge [2] and spin [3, 4, 5] degrees of freedom. Scale-up, however, requires more than the ability to fabricate many qubits and the associated nanoelectronics. In Ref. [8] a scalable donor electron spin qubit architecture was proposed based on a bi-linear arrangement of qubits. A key feature of this architecture is a transport mechanism using Coherent Tunneling Adiabatic Passage (CTAP) [6] which both allows for qubit transport during quantum error correction and serves to reduce the effective gate density of the nanoelectronics. CTAP is a spatial analogue of the well known STIRAP protocol [7] from quantum optics for coherent transfer of quantum information. The advantage of CTAP is that it affords long-range, flexible and robust transfer as is required for scale up of donor based architectures.

In addition to phosphorus in silicon, there are proposals to observe CTAP in quantum dots [9, 10], superconductors [11], single atoms in optical potentials [12, 13], and Bose-Einstein Condensates [14, 15]. Recently Longhi et al. [16, 17, 18] demonstrated CTAP of photons in a three-waveguide structure adding significant motivation to demonstrations with massive particles. CTAP has also been proposed as a means of implementing a quantum analogue to fanout using MRAP (Multi-Recipient Adiabatic Passage) [19, 20] and operator measurements. Other recent works have investigated the differences in CTAP in quantum optics and solid state systems [21, 22]. Atomistic simulations of triple donor systems in silicon have been investigated [23], verifying the existence of an CTAP pathway for a small three donor device and the use of ion-implantation for fabrication of CTAP devices have been discussed Ref. [24]. Triple dots have recently also been demonstrated in GaAs 2DEG structures [25, 26, 27] and carbon nanotubes [28].

The transport protocols discussed in [6, 8] were based on the straddling scheme introduced by Malinovsky and Tannor [29] where two sites are coupled to the ends of a strongly coupled and uncontrolled chain. Providing that the tunneling matrix elements between sites on the chain are significantly higher than the gate controlled tunneling matrix elements (TMEs) of the end-of-chain sites, then the protocol works by transporting the particle between the end-of-chain sites with negligible population ever appearing along the intermediate sites in the chain (even transiently).

In this paper we consider a different adiabatic protocol suitable for long range (multi-site) transport based on the alternating scheme. This was proposed in the context of quantum dot transport of electrons by Petrosyan and Lambropolous [9] and is also known for STIRAP protocols [30] Here we consider this scheme for the case of phosphorus ions in silicon.

Successful coherent transfer of the electron across the chain requires the protocol to be completed within the charge relaxation time, and in order to be useful for spin based quantum computing architectures must also be within the qubit spin dephasing time, T_2. Recent measurements of electron spin relaxation for phosphorus donors in purified Si^{28} have yielded a T_2 of approximately 60ms at 7K [31] and still in the millisecond range when the donors are placed near a surface or interface [32] . Charge dephasing in a Si:P-P^+ system have been investigated in Refs. [33, 34], estimating the

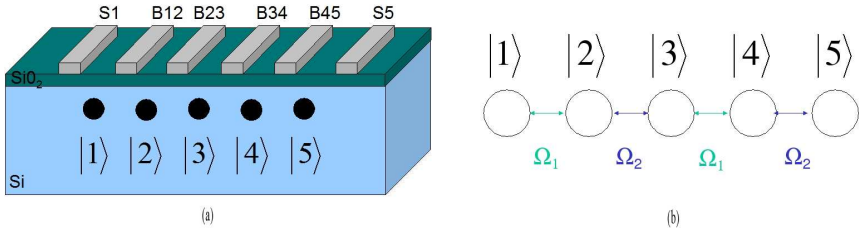

Figure 1: (a) Schematic of a five donor, one electron device for CTAP using the alternating coupling scheme. Barrier gates (B_{ij}) control the tunneling of the electron between buried phosphorus donor sites. (b) The counter intuitive coupling scheme. Tunneling matrix elements in the five site chain are controlled as an A-B chain. The counter-intuitive pulse sequence applies all of the Ω_2 tunneling before Ω_1 tunneling to effect transport from $|1\rangle$ to $|5\rangle$.

dephasing time to be of order nanoseconds.

We consider a five donor structure, illustrated in Figure 1(a), where four donors are ionized and one is neutral. Gates on the surface control the tunnel matrix elements and thereby define the adiabatic pathway for electronic transport. The counter-intuitive, alternating gate bias sequence, illustrated in figure 1(b), varies the tunnel matrix elements resulting in robust transport of the electron from one end of the chain to the other. This structure is extendable to an arbitrary (odd) number of sites. Based on an effective mass treatment we analyse the system and make estimates of the timescale required for the operation of CTAP with the alternating coupling scheme for this device.

2. Analytics

We begin by writing down the analytical form of the null space for the problem with $2n+1$ states for a single particle. We assume that the TME between states is $|2i-1\rangle$ and $|2i\rangle$ is Ω_i, and that all of the even Ω_i and the odd Ω_i can be controlled separately from 0 to some maximum value. Note that we are here explicitly using the modal approximation. Recent calculations have shown this to be a very good approximation for CTAP problems [15, 21, 22, 23] although the exact nulling of some central state populations that is predicted for CTAP does *not* precisely occur for realistic potentials. Assuming that the energies of the states are all degenerate, we write down the Hamiltonian as:

$$\mathcal{H} = \sum_{i=1}^{n} \Omega_{2i-1}|2i-1\rangle\langle 2i| + \Omega_{2i}|2i\rangle\langle 2i+1| + \text{h.c.} \tag{1}$$

We can immediately write down the null space solution, which we write as $|\mathcal{D}_0\rangle = \sum_{i=1}^{2n+1} \psi_i|i\rangle$. First note that all of the ψ at even sites must vanish, i.e. $\psi_{2i} = 0$. Secondly we can write down the values of the ψ at odd sites as a series, i.e.

$$\psi_{2i+1} = -\frac{\Omega_{2i-1}}{\Omega_{2i}}\psi_{2i-1}, \tag{2}$$

and hence

$$\psi_{2i+1} = (-1)^i \prod_{j=1}^{j=i} \left(\frac{\Omega_{2j-1}}{\Omega_{2j}}\right) \psi_1. \tag{3}$$

We may now write down the normalisation to get the correct form of the null vector, $|\mathcal{D}_0\rangle$, which is

$$|\mathcal{D}_0\rangle = \frac{1}{N}\left(\prod_{i=1}^{n}\Omega_{2i}|1\rangle + \cdots + (-1)^j \prod_{i=j}^{n}\Omega_{2i}\prod_{i=1}^{j}\Omega_{2i-1}|2j+1\rangle + \cdots + (-1)^n \prod_{i=1}^{n}\Omega_{2i-1}|2n+1\rangle\right) \tag{4}$$

with

$$N = \left[\left(\prod_{i=1}^{n}\Omega_{2i}\right)^2 + \cdots + \left(\prod_{i=j}^{n}\Omega_{2i}\prod_{i=1}^{j}\Omega_{2i-1}\right)^2 + \cdots + \left(\prod_{i=1}^{n}\Omega_{2i-1}\right)^2\right]^{1/2} \tag{5}$$

This form for $|\mathcal{D}_0\rangle$ immediately shows that this null space has all the desired properties. It is unidimensional, when the odd TMEs are all zero and the even TMEs all non-zero, the system is in $|1\rangle$, and when the even TMEs are all zero with the odd non-zero, the system is in state $|2n+1\rangle$, with a smooth adiabatic pathway between the states. Apart from enforcing the zeros of the tunneling matrix element no control as the *relative* values is required. In fact, this adiabatic pathway is maintained provided that only the *ends* of the alternating pathway can be satisfactorily nulled, ie that $\Omega_1 = 0$ at t=0 and $\Omega_{2n} = 0$ at $t = t_{max}$, which makes the protocol an attractive prospect for implementing as less fine controls are required, decreasing the amount of gates and connections required.

Considering the $|\mathcal{D}_0\rangle$ for a five site system ($ACTAP_5$) explicitly we have:

$$|\mathcal{D}_0^{(5)}\rangle = \frac{\Omega_2\Omega_4|1\rangle - \Omega_1\Omega_4|3\rangle + \Omega_1\Omega_3|5\rangle}{\sqrt{(\Omega_2\Omega_4)^2 + (\Omega_1\Omega_4)^2 + (\Omega_1\Omega_3)^2}}. \tag{6}$$

We see that when Ω_1 is zero, there is only population in $|\mathcal{D}_0\rangle = |1\rangle$. Similarly, when Ω_4 is zero, the null state is $|\mathcal{D}_0\rangle = |5\rangle$ does not depend on Ω_2. This allows us to consider global controls of all the even tunneling matrix elements together and similarly for all the odd elements, with only the need to fine tune the ends of the chain, Ω_1 and Ω_4 in the $ACTAP_5$ case. Global controls, and specifically A-B chains as we are discussing here, have been investigated in the context of Heisenberg chains [35].

Another important feature of equation 6 is that it illustrates the robustness of the ACTAP protocol to fabrication errors. In particular, one should note the existence of the null state irrespective of the values of the TMEs, providing that they can be varied between zero and finite values. This is useful when considering the limitations of conventional fabrication techniques, e.g. single ion implantation [36] which will have unavoidable variability in the final positions of the donors due to straggle. As only the ratios of the TMEs enter into the form of the null state, the adiabatic pathway persists in the presence of such variations in site to site coupling. It is important to note that the adiabaticity of the protocol, and hence the time taken for high-fidelity transport, will vary also, and so any given device will need to be calibrated. Further discussions on the role of TME variability in related CTAP protocols can be found in [8, 23, 24].

For simplicity let us now consider the case where all the odd tunnel matrix elements are the same, and the even ones also, i.e.

$$\Omega_{2i-1} = \Omega_1 \text{ and } \Omega_{2i} = \Omega_2 \ \forall i, \tag{7}$$

and concentrating on ACTAP_5 we have the following result for the null state:

$$|\mathcal{D}_0^{(5)}\rangle = \frac{\Omega_2^2|1\rangle - \Omega_1\Omega_2|3\rangle + \Omega_1^2|5\rangle}{\sqrt{\Omega_1^4 + \Omega_2^4 + \Omega_1^2\Omega_2^2}}. \tag{8}$$

Furthermore we can also determine all of the eigenstates and eigenvalues for this symmetric case. The eigenstates are

$$|\mathcal{D}_0^{(5)}\rangle = \frac{\Omega_2^2|1\rangle - \Omega_1\Omega_2|3\rangle + \Omega_1^2|5\rangle}{\sqrt{\Omega_1^4 + \Omega_2^4 + \Omega_1^2\Omega_2^2}}, \tag{9}$$

$$\begin{aligned}|\mathcal{D}_\pm^{(5)}\rangle = &[-\Omega_1|1\rangle \mp \sqrt{\Omega_1^2 - \Omega_1\Omega_2 + \Omega_2^2}(|2\rangle - |4\rangle) \\ + \quad &(\Omega_1 - \Omega_2)|3\rangle + \Omega_2|5\rangle)][2\sqrt{\Omega_1^2 - \Omega_1\Omega_2 + \Omega_2^2}]^{-1},\end{aligned} \tag{10}$$

$$\begin{aligned}|\mathcal{D}_{2\pm}^{(5)}\rangle = &[\Omega_1|1\rangle \pm \sqrt{\Omega_1^2 + \Omega_1\Omega_2 + \Omega_2^2}(|2\rangle + |4\rangle) \\ + \quad &(\Omega_1 + \Omega_2)|3\rangle + \Omega_2|5\rangle)][2\sqrt{\Omega_1^2 + \Omega_1\Omega_2 + \Omega_2^2}]^{-1},\end{aligned} \tag{11}$$

with eigenenergies

$$E_0 = 0, \tag{12}$$

$$E_\pm = \pm\sqrt{\Omega_1^2 - \Omega_1\Omega_2 + \Omega_2^2}, \tag{13}$$

$$E_{2\pm} = \pm\sqrt{\Omega_1^2 + \Omega_1\Omega_2 + \Omega_2^2}. \tag{14}$$

To explore the evolution of the system, for analytical simplicity we chose square sinusoidal pulse variation of Ω_1 and Ω_2, however in keeping with most adiabatic protocols, the exact form of the variation in tunneling matrix elements is not essential. For pulses from $t = 0$ to $t = t_{\max}$ we set:

$$\Omega_1 = \Omega_{\max}\sin^2\left(\frac{\pi t}{2t_{\max}}\right), \tag{15}$$

$$\Omega_2 = \Omega_{\max}\cos^2\left(\frac{\pi t}{2t_{\max}}\right), \tag{16}$$

and these pulses are illustrated in Figure 2(a).

The null state is the eigenstate which has zero energy throughout the protocol. This is the state used for the CTAP protocol, as its evolution under the pulse sequence gives rise to a smooth change in population from $|1\rangle$ at $t = 0$ to $|5\rangle$ at $t = t_{\max}$. We can then find the eigenvalues for this Hamiltonian, shown plotted in figure 2(b). Solving the master equation for this Hamiltonian, we obtain the occupancies of each of the donor sites throughout the protocol. Analogously with other CTAP protocols, we treat the electron as initially occupying the first site, and transferred entirely to the end-of-chain site at the end of the protocol. In the alternating scheme there is transient occupation of the site in the middle of the chain, as shown in Figure 2(c) but other intermediate sites remain unoccupied. This differs from the straddling scheme [6, 8] where occupation of all intermediate sites is strongly suppressed.

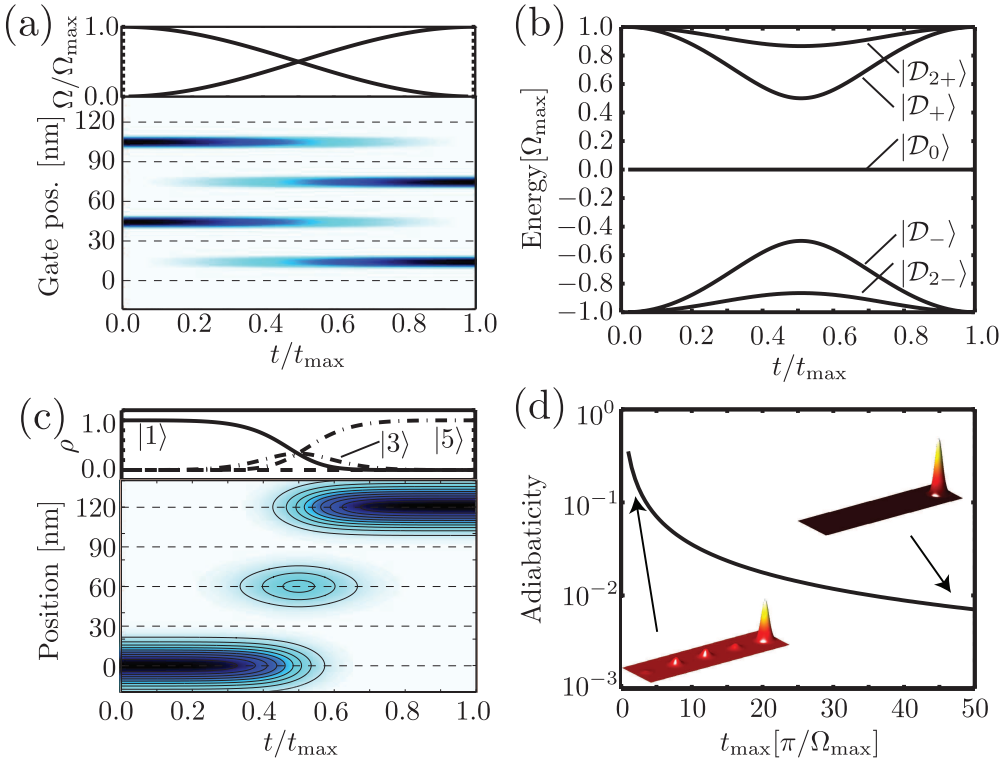

Figure 2: (a) The top trace shows the TMEs Ω_1 and Ω_2 as a function of time. Below, the TMEs between donors (postions marked by dashed lines) are illustrated as a density plot as a function of time. TMEs controlled by gates 2 and 4 are high initially (Ω_2), whilst the TMEs controlled by gates 1 and 3 are low initially (Ω_1). Varying the biases on the gates effects the counter-intuitive pulse sequence described. (b) Eigenvalue spectrum of the $ACTAP_5$ Hamiltonian . (c) Populations of the position eigenstates throughout the protocol. Note the complete transfer from $|1\rangle$ to $|5\rangle$ but with transient population in $|3\rangle$, and no population in either $|2\rangle$ or $|4\rangle$. (d) Adiabaticity as $t_{\max}$ increases. As $t_{\max}$ is increased the adiabaticity parameter is decreased indicating better fidelity tranfer across the chain. A shorter total time for the protocol can to transitions out of the $|\mathcal{D}_0\rangle$ state and the transfer of the electron from $|1\rangle$ to $|5\rangle$ is no longer complete.

The Adiabaticity parameter can be fairly easily calculated between the null state and either of the nearest neighbours, so in particular, choosing the closest positive state, we write the Adiabaticity parameter as

$$\mathcal{A} = \frac{|\langle \mathcal{D}_+ | \frac{\partial \mathcal{H}}{\partial t} | \mathcal{D}_0 \rangle|}{|E_+ - E_0|^2}, \tag{17}$$

$$= \frac{\dot{\Omega}_1 \Omega_2^2 - \dot{\Omega}_2 \Omega_1^2 + \Omega_1 \Omega_2 (\dot{\Omega}_1 - \dot{\Omega}_2)}{2\sqrt{\Omega_1^4 + \Omega_1^2 \Omega_2^2 + \Omega_2^4}(\Omega_1^2 - \Omega_1 \Omega_2 + \Omega_2^2)} \tag{18}$$

For adiabatic evolution we require that $\mathcal{A} \ll 1$ with the maximal adiabaticty determining the time allowable for a realistic experiment. If we note that the

adiabaticity parameter will be largest at the crossing point of the two TMEs, and if we apply pulses that are symmetric, then we can make a considerable simplification to the above. So at the point where $\mathcal{A}$ is greatest, we have $\Omega_1 = \Omega_2 = \Omega_{\max}/2$, and $\dot{\Omega}_1 = \dot{\Omega}_2 = \pi\Omega_{\max}/(2t_{\max})$ and we find using the form of the TMEs as given in equation 15, the above equation gives rise to the simple form

$$\mathcal{A} = \frac{4\pi}{\sqrt{3}\Omega_{\max}t_{\max}}. \tag{19}$$

This dependence of the adiabaticity parameter on the the total protocol time $t_{\max}$is plotted in Figure 2(d). With longer $t_{\max}$, and hence lower $\mathcal{A}$, the transported electron is more likely to remain in the desired $|\mathcal{D}_0\rangle$ state resulting in better fidelity transfer.

A realistic device may not have enough fine control over the TMEs to be able to completely turn them on or off. In this case we have non-zero minimum values and assuming a form for the TMEs of:

$$\Omega_1(t) = \Omega_{1\,\min} + (\Omega_{1\,\max} - \Omega_{1\,\min})\sin^2\left(\frac{\pi t}{2t_{\max}}\right), \tag{20}$$

$$\Omega_2(t) = \Omega_{2\,\min} + (\Omega_{2\,\max} - \Omega_{2\,\min})\cos^2\left(\frac{\pi t}{2t_{\max}}\right). \tag{21}$$

In the case where complete suppression of the tunneling is not possible, a measure of our ability to turn off tunneling between donors is the contrast ratio between the overlap of the initial and final states with $|\mathcal{D}_0\rangle$. The contrast ratio defines an error rate for the protocol when we do not have complete suppression of the tunneling. For a device to successfully perform the protocol we require the contrast ratio to be high, reaching a maximum of 1 when complete suppression is possible. This can be determined by calculating the product of the overlap $\langle 1|\mathcal{D}_0\rangle$ at $t = 0$ and $\langle \mathcal{D}_0|5\rangle$ at t=$t_{\max}$.

$$\langle 1|\mathcal{D}_0(t=0)\rangle = \frac{\Omega_{2\,\max}^2}{\sqrt{\Omega_{1\,\min}^4 + \Omega_{2\,\max}^4 + \Omega_{1\,\min}^2\Omega_{2\,\max}^2}}, \tag{22}$$

and assuming $\Omega_{1\,\min} \ll \Omega_{2\,\max}$, to first order:

$$\langle 1|\mathcal{D}_0(t=0)\rangle = 1 - \frac{\Omega_{1\,\min}^2}{2\Omega_{2\,\max}^2}. \tag{23}$$

Similarly, at the end of the protocol, when $t = t_{\max}$ the null state is:

$$\langle \mathcal{D}_0(t=t_{\max})|5\rangle = \frac{\Omega_{1\,\max}^2}{\sqrt{\Omega_{2\,\min}^4 + \Omega_{1\,\max}^4 + \Omega_{2\,\min}^2\Omega_{1\,\max}^2}}. \tag{24}$$

Applying the same approximations as before gives the result:

$$\langle \mathcal{D}_0(t=t_{\max})|5\rangle = 1 - \frac{\Omega_{2\,\min}^2}{2\Omega_{1\,\max}^2}, \tag{25}$$

so a first approximation to the fidelity of population transfer in this case of imperfect contrast ratio is

$$|\langle 5|\mathcal{D}_0(t=t_{\max})\rangle\langle \mathcal{D}_0(t=0)|1\rangle|^2 = 1 - \frac{\Omega_{1\,\min}^2\Omega_{2\,\min}^2}{8\Omega_{1\,\max}^2\Omega_{2\,\max}^2}. \tag{26}$$

To illustrate with an example, to achieve a fidelity of 99.9% and assuming that $\Omega_1 = \Omega_2$, we require a ratio of $\Omega_{\min}/\Omega_{\max} = 0.3$, hence we can see that a high fidelity transfer may still be possible, even with imperfect controls.

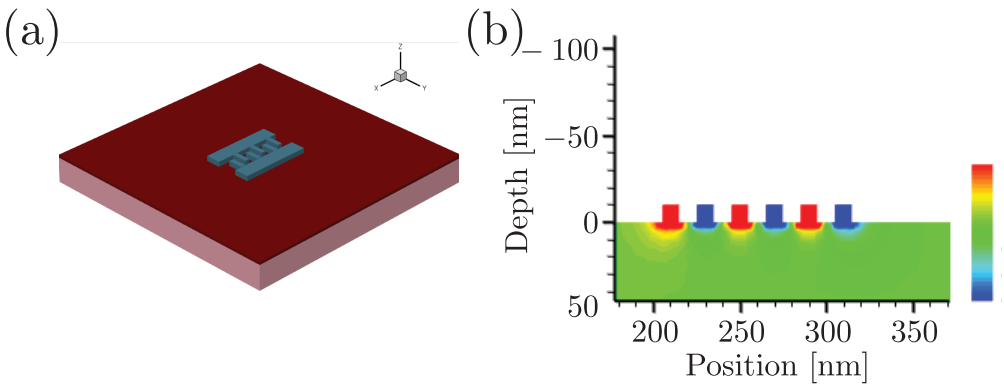

Figure 3: a) An interdigitated gate design for A-CTAP. Donors are placed in between gate "fingers" in the central region of the device. All odd gates are connected together and similarly for all the even gates. b) A slice taken from a TCAD simulation of potentials within the device, slicing through the centre of all the donors which are located in a line parallel to the position axis.

We now turn our attention to calculating the gate modulated tunnel matrix elements for a semi-realistic 5 donor device which we will use with the above expressions for adiabaticity and fidelity to estimate the timescale of the protocol over such a device.

3. Numerical Modeling

The increased simplicity of an alternating coupling scheme over other schemes makes it an attractive candidate for possible implementation for demonstrating CTAP in a Si:P setting. Figure 3 illustrates a possible gate design to implement ACTAP_5. This design features global control of the even and odd tunneling matrix elements with even and odd barrier gates connected to be pulsed together. These global controls are desirable due to the simpler fabrication and reduced control circuitry required. Fine tuning of the end of chain sites may be implemented using further gates but they are not included here. Modeling of the potentials within the device with applied gate biases was performed using a commercial TCAD finite element modeling package. A simulation of the correct gate voltage sequence required to enact the CTAP protocol is a difficult control problem with cross-talk effects needing to be taken into account. Compensation schemes for gated donor schemes have been investigated in Ref. [37] and similar measures may need to be implemented here to ensure the correct tunnel matrix elements are obtained. We apply here a simpler approach of looking at pairwise tunneling rates with a simplified structure consisting of two donors and a barrier gate to modulate tunneling rates.

The phosphorus in silicon scheme we are considering consists of ionised ^{31}P buried in a ^{28}Si substrate. Each of the ionised phosphorus atoms forms bonds with neighbouring silicon atoms with their remaining 4 valence electrons. One un-ionised donor remains in the chain with a remaining valence electron loosely bound to the donor. This remaining electron's wavefunction may be manipulated using surface gates to effect the transport across the chain.

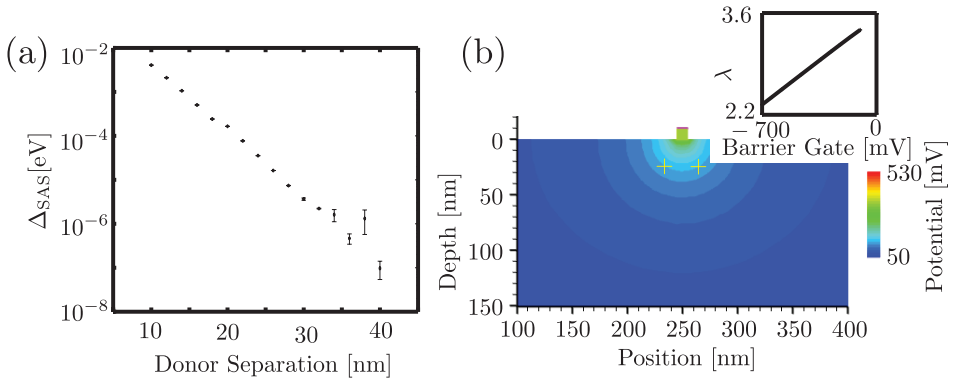

Figure 4: (a) Ungated Δ_{SAS} as a function of donor separation in [100]. As donors are moved further apart the tunneling rate between them is decreased. The large fluctations at large donor separations are due to fluctations in the Monte Carlo routine. (b) A slice taken from a TCAD simulation of the simplified, one gate, two donor device. The slice in the vertical plane of the two donors. The 10 nm wide gate is centred about 250 nm directly between the positions of the two donors placed 30 nm apart, as marked by the crosses in the picture. (Inset) Relationship between fitted charge density and TCAD obtained fields. Note the linear fit. Errors in the value of λ obtained were $\pm 0.01\%$.

The electronic states of shallow donors in silicon have been well studied. To calculate the energy states of the remaining valence electron we use the effective mass approach developed by Kohn and Luttinger [38] in which the donor electron is described using hydrogenic envelope functions. This approach is extended to include a second ionised donor such that the electron is described by symmetric and anti-symmetric superpositions of the ground state for each donor and an external electric field. The effective Hamiltonian for the two donor, Si:P-P^+ system is given by:

$$\mathcal{H} = \mathcal{H}_{\rm si} + V_d(r - R_1) + V_d(r - R_2) + V_E \tag{27}$$

where $H_{\rm Si}$ is the Hamiltonian of an electron in the pure silicon lattice, which includes both a kinetic term and the effective potential due to the silicon lattice, V_d the coulombic potentials of each donor and V_E an external applied field [39, 40, 41]. The valence electron can be described by symmetric and anti-symmetric superpositions of the ground state of each for each separate donor:

$$\Psi_{\pm}(\mathbf{r}) = \mathcal{N}[\psi(\mathbf{r} - \mathbf{R}_\alpha) \pm \psi(\mathbf{r} - \mathbf{R}_\beta)] \tag{28}$$

where $\mathcal{N}$ is a normalisation factor and the the ground state for a single phosphorus donor centred about R_α is given by:

$$\psi(r) = \sum_{\mu=1}^{6} F_\mu(r - R) e^{\imath k_\mu \cdot (r - R_\alpha)}. \tag{29}$$

The $F_\mu(r - R)$ are effective mass, hydrogenic envelope functions about the six degenerate band minima.

TMEs may then be calculated by examining the minimum energy splitting between the lowest energy states of a donor pair, the symmetric-antisymmetric gap

$\Delta_{\rm SAS}$. TMEs may then be varied from $\Omega_{\rm max} = \Delta_{\rm SAS}$ to 0 using time varying gate bias pulses such as those described in equations 15 and 16. Examining these gate driven couplings gives an indication of the timescale of the tunneling rates, and hence the timescale of the protocol.

Figure 4 shows the calculated $\Delta_{\rm SAS}$ as a function of donor spacing for a P-P^+ system with no external field is applied. At 30nm $\Delta_{\rm SAS}$ is calculated as 0.1μeV, corresponding to a tunneling matrix element of $\sim$ 2 GHz. These calculations are consistent with the hydrogenic results of Openov [42] To include the effect of the external field on the tunneling rate we have utilised an analytic potential fitted to the potential landscapes obtained from several TCAD simulations at different gate biases. This approach allows us to use a simple form for the external field which varies smoothly over space which can be varied with any possible gate potential while maintaining a close connection to modeling of semi-realistic structures. In the y-z plane we approximate the surface gate with an infinite line of charge the same distance above the ground plane with the origin at the line of charge. Using the method of images we obtain the form of the potential:

$$V = \frac{\lambda}{2\pi\epsilon_0\epsilon_r} \ln \frac{y^2 + (z+d)^2}{y^2 + (z-d)^2} \tag{30}$$

where λ is the charge density of the line of charge obtained using the simulated TCAD potentials, shown in figure 4(b)Inset and d is the distance of the line of charge above the ground plane. Since the dielectric constant of the SiO_2 is much less than that of the bulk silicon, the discontinuity in the resulting field is accounted for by extending the 5nm oxide layer to an equivalent thickness with a bulk silicon dielectric constant to ensure the correct field in the bulk silicon is obtained. This relationship between λ and barrier gate voltage has a constant offset due to the contact potential of around 0.5 V that arises from the aluminium gates placed on the silicon dioxide layer. Since we are only interested in the effect net effect of the gate we have ommitted this constant offset in the calculation of $\Delta_{\rm SAS}$ so zero volts corresponds to the field-free (ie purely hydrogenic) case. In practice this would be achieved by the gate offsetting the surface charge.

Figure 5 shows the calculated variation of $\Delta_{\rm SAS}$ with barrier gate voltage. We see a variation in $\Delta_{\rm SAS}$ from $\sim$ 0.5 to 10 GHz with a change of approximately 250 mV applied voltage on the barrier gate. This is consistent, within uncertainty, with previous modelling of the energy gap for P-P^+ charge qubit with donor spacing of 30nm, showing that tunneling may be varied from around 0 to 10 GHz with a change in barrier gate bias of 300 mV [8]. The errors in $\Delta_{\rm SAS}$ are dominated by fluctuations in v_z due to sampling errors in the Monte Carlo routine. Using equation 26 with $\Omega_{\rm min} = 0.5$GHz and $\Omega_{\rm max} = 10$GHz and assuming $\Omega_1 = \Omega_2$ we obtain an error rate of 10^{-6}. This result demonstrates the remarkable robustness of the protocol to imperfect control of the tunneling matrix elements. Ideally v_z is 0 when the field is completely symmetric with respect to the two donors and consists of the diagonal elements of the external field component of the Hamiltonian cancelling with each other. If we neglect v_z in calculating $\Delta_{\rm SAS}$ we obtain a minimum tunneling rate of around 0.1GHz and an error rate of 10^{-8}.

Assuming perfect contrast, for a target adiabaticity of 0.01 we may now calculate the required time for the protocol. Using equation 19, with $\Omega_{\rm max}$=10GHz we obtain $t_{\rm max} \sim 70$ns as the required time for adiabatic transfer of an electron across the chain, in this case 120nm long.

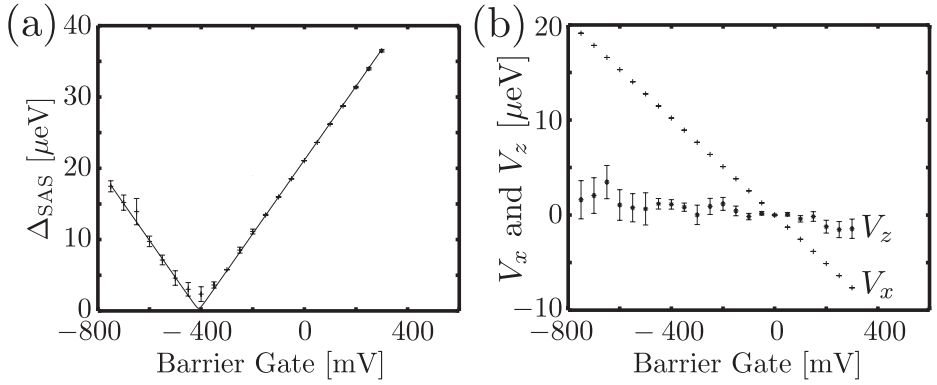

Figure 5: (a)Variation of $\Delta_{\rm sas}$ with applied barrier gate voltage. We see a variation in $\Delta_{\rm sas}$ from 0.5 to 10 GHz in a change of approximately 250 mV applied voltage on the barrier gate. The larger errors at larger spacings are due to the Monte Carlo routine. (b) v_x and v_z coefficients as a function of barrier gate voltage. The fluctations in v_z are due to sampling errors in the Monte Carlo routine.

Allowing for a large range variablity in the TMEs while still being able to obtain high fidelity transfer of the electron means that the protocol is also robust to donor placement. Variations to donor placement will result in variations in the ungated TMEs as shown in Figure 4. However, as shown in equation 26, adiabatic behaviour will still occur over a wide range of maximum and minimum TMEs. As a result the protocol can be insensitive to variations in donor placement, which is important since devices such as this proposed are generally fabrication using ion implantation techniques where there is variability in the exact placement of the donor.

4. Conclusion

We have shown that for a semi-realistic device consisting of buried phosphorus donors in silicon with surface gates, an adiabatic pathway may be found allowing transport of quantum information along a donor chain using the alternating coupling scheme. The fidelity of the transport protocol is resilient to variations in the TMEs along the chain so long as the end-of-chain sites can be controlled. We calculate that, for a device with a relatively large donor spacing of 30nm, with a maximum pairwise tunneling rate of 10 GHz which can be suppressed to 0, we can estimate a time of ~ 70 ns required for adiabatic operation. For closer positioned donors we expect an adiabatic operation time down to the few nanosecond regime or faster. This time is well within measured electron spin relaxation times and dephasing for silicon and within the expected charge relaxation times for Si:P devices.

Acknowledgments

This work was supported by the Australian Research Council Centre of Excellence Scheme, the Australian Government and by the US National Security Agency (NSA), Advanced Research and Development Activity (ARDA) and the Army Research Office (ARO) under Contract No. W911NF-04-1-0527. ADG is the recipient of an Australian

Research Council Queen Elizabeth II Fellowship (project number DP0880466), LCLH is the recipient of an Australian Research Council Australian Professorial Fellowship (project number DP0770715).

References

[1] B. E. Kane, "A silicon-based nuclear spin quantum computer", Nature (Lond) 393, 133 (1998).
[2] L. C. L. Hollenberg, A. S. Dzurak, C. Wellard, A. R. Hamilton, D. J. Reilly, G. J. Milburn, R. G. Clark, "Charge-based quantum computing using single donors in semiconductors", Phys. Rev. B 69, 113301 (2004).
[3] R. Vrijen, E. Yablonovitch, K. Wang, H.W. Jiang, A. Balandin, V. Roychowdhury, T. Mor and D. Divincenzo, "Electron-spin-resonance transistors for quantum computing in silicon-germanium heterostructures", Phys. Rev. A 62, 012306 (2000).
[4] C. D. Hill, L. C. L. Hollenberg, A. G. Fowler, C. J. Wellard, A. D. Greentree and H. -S. Goan, "Global control and fast solid-state donor electron spin quantum computing", Phys. Rev. B, 72, 045450 (2005).
[5] R. de Sousa, J.D. Delgado and S. Das Sarma, "Silicon quantum computation based on magnetic dipolar coupling", Phys. Rev. A 70, 052304 (2004).
[6] A.D. Greentree, J.H. Cole, A.R. Hamilton, and L.C.L. Hollenberg, "Coherent electronic transfer in quantum dot systems using adiabatic passage", Phys. Rev. B 70, 235317 (2004).
[7] V. Vitanov, T. Halfmann, B.W. Shore and K. Bergmann, "Laser-induced population transfer by adiabatic passage techniques.", Annu. Rev. Phys. Chem. 52, 763 (2001).
[8] L.C.L. Hollenberg, A.D. Greentree, A.G. Fowler, and C.J. Wellard, "Two-dimensional architectures for donor-based quantum computing", Phys. Rev. B 74, 045311 (2006).
[9] D. Petrosyan and P. Lambropoulos, "Coherent population transfer in a chain of tunnel coupled quantum dots", Optics Communications 264 419 (2006).
[10] D. Schröer, A.D. Greentree, L. Gaudreau, K. Eberl, L.C.L. Hollenberg, J.P. Kotthaus and S. Ludwig, "Electrostatically defined serial triple quantum dot charged with few electrons", Phys. Rev. B 76, 075306 (2007).
[11] J. Siewert, T. Brandes, and G. Falci, "Adiabatic passage with superconducting nanocircuits", Optics Comm. 264, 435 (2006).
[12] K. Eckert, M. Lewenstein, R. Corbaln, G. Birkl, W. Ertmer, and J. Mompart, "Three-level atom optics via the tunneling interaction", Phys. Rev. A 70, 023606 (2004).
[13] K. Eckert, J. Mompart, M. Lewenstein, R. Corbaln and G. Birkl, "Three level atom optics in dipole traps and waveguides", Optics Comm. 264, 264 (2006).
[14] E. M. Graefe, H. J. Korsch, and D. Witthaut, "Mean-field dynamics of a Bose-Einstein condensate in a time-dependent triple-well trap: Nonlinear eigenstates, Landau-Zener models, and stimulated Raman adiabatic passage", Phys. Rev. A 73, 013617 (2006).
[15] M. Rab, J.H. Cole, N.G. Parker, A.D. Greentree, L.C.L. Hollenberg, and A. M. Martin, "Matterwave Transport Without Transit",Phys. Rev. A 77, 061602(R) (2008).
[16] S. Longhi, "Photonic transport via chirped adiabatic passage in optical waveguides", J. Phys. B: At. Mol. Opt. Phys. 40 F189-F195 (2007).
[17] S. Longhi, G. Della Valle, M. Ornigotti, and P. Laporta, "Coherent tunneling by adiabatic passage in an optical waveguide system", Phys. Rev. B 76, 201101 (2007).
[18] G. Della Valle, M. Ornigotti, T. Toney Fernandez, P. Laporta, and S. Longhi, "Adiabatic light transfer via dressed states in optical waveguide arrays",Appl. Phys. Lett. 92, 011106 (2008).
[19] A. D. Greentree, S. J. Devitt and L. C. L. Hollenberg, "Quantum-information transport to multiple receivers", Phys. Rev. A 73, 032319 (2006).
[20] S.J. Devitt, A.D. Greentree and L.C.L Hollenberg, "Information free quantum bus for generating stabilized states", Quant. Inf. Proc. 6, 229 (2007).
[21] J.H. Cole, A.D. Greentree, S. Das Sarma, and L.C.L. Hollenberg, "Spatial adiabatic passage in a realistic triple well structure", Phys. Rev. B 77, 235418 (2008).
[22] T. Opatrný and K.K. Das, "Conditions for Vanishing Central-well Population in Triple-well Adiabatic Transport", Phys. Rev. A 79, 012113 (2009).
[23] R. Rahman, S.H. Park, J.H. Cole, A. D. Greentree, R. P. Muller, G. Klimeck and L. C.L. Hollenberg,"Atomistic simulations of adiabatic coherent electron transport in triple donor systems", Phys. Rev. B 80 035302 (2009).
[24] J. A. Van Donkelaar, A. D. Greentree, L. C. L. Hollenberg and D. N. Jamieson, "Strategies for triple-donor devices fabricated by ion implantation",arXiv:0806.2691 (2008).
[25] L. Gaudreau S. A. Studenikin, A. S. Sachrajda, P. Zawadzki, A. Kam, J. Lapointe, M.

Korkusinski, and P. Hawrylak,"Stability Diagram of a Few-Electron Triple Dot", Phys. Rev. Lett. 97, 036807 (2006).
[26] M.C. Rogge and R.J. Haug, "Two-path transport measurements on a triple quantum dot", Phys. Rev. B. 77, 193306 (2008).
[27] S. Amaha, T. Hatano, T. Kubo, S. Teraoka, Y. Tokura, S. Tarucha, and D. G. Austing, "Stability diagrams of laterally coupled triple vertical quantum dots in triangular arrangement", Appl. Phys. Lett. 94, 092103 (2009).
[28] K. Grove-Rasmussen, H. I. Jørgensen, T. Hayashi, P. E. Lindelof, and T. Fujisawa, "A triple quantum dot in a single-wall carbon nanotube", Nano Lett. 8, 1055, (2008).
[29] S. Malinovsky and D. J. Tannor, "Simple and robust extension of the stimulated Raman adiabatic passage technique to N-level systems", Phys. Rev. A 56, 4929 (1997).
[30] B.W. Shore, K. Bergmann, J. Oreg and S. Rosenwalks, "Multilevel adiabatic population transfer", Phys. Rev. A 44, 7442 (1991).
[31] A.M. Tyryshkin, S.A. Lyon, A.V. Astashkin, and A.M. Raitsimring, "Electron spin relaxation times of phosphorus donors in silicon", Phys. Rev. B. 68, 193207 (2003).
[32] A.M. Tyryshkin, S.A. Lyon, T. Schenkel, J. Bokor, J. Chu, W. Jantsch, F. Schäffler, J.L. Truitt, S.N. Coppersmith, M.A. Eriksson, "Electron spin coherence in Si", Physica E 35 257 (2006)
[33] S.D. Barrett and G.J. Milburn, "Measuring the decoherence rate in a semiconductor charge qubit", Phys. Rev. B. 68, 155307 (2003).
[34] J. Gorman, D.G. Hasko and D.A. Williams, "Charge-Qubit Operation of an Isolated Double Quantum Dot", Phys. Rev. Lett. 95, 090502 (2005).
[35] S.C. Benjamin, "Quantum computing without local control of qubit-qubit interactions", Phys. Rev. Lett. 88, 17904 (2002).
[36] D. N. Jamieson, C. Yang, T. Hopf, S. M. Hearne, C. I. Pakes, S. Prawer, M. Mitic, E. Gauja, S. E. Andresen, F. E. Hudson, A. S. Dzurak, and R. G. Clark, "Controlled shallow single-ion implantation in silicon using an active substrate for sub-20-keV ions", Appl. Phys. Lett. 86, 202101 (2005)
[37] G. Kandasamy, C.J. Wellard and L.C.L. Hollenberg, "Cross-talk compensation of hyperfine control in donor-qubit architectures", Nanotechnology 17, 4572 (2006).
[38] W. Kohn and J.M. Luttinger, "Theory of Donor States in Silicon", Phys. Rev. 98, 915 (1955).
[39] B. Koiller, X. Hu and S. Das Sarma, "Electric-field driven donor-based charge qubits in semiconductors", Phys. Rev. B 73, 045319 (2006).
[40] C.J. Wellard, L.C.L. Hollenberg and S. Das Sarma,"Theory of the microwave spectroscopy of a phosphorus-donor charge qubit in silicon: Coherent control in the Si:P quantum-computer architecture", Phys. Rev. B 74, 075306 (2006).
[41] V.I. Conrad, "Designing a Solid-State Qubit: Computational modeling of two level quantum systems in silicon and associated nano-electrons.", PhD Thesis (2007).
[42] L.A. Openov, "Resonant pulse operations on the buried donor charge qubits in semiconductors", Phys. Rev. B 70, 233313 (2004)